RSC Advances

PAPER

View Article Online
View Journal | View Issue

Cite this: *RSC Adv.*, 2017, **7**, 21638

Heterogeneous Fenton-like degradation of phenanthrene catalyzed by schwertmannite biosynthesized using *Acidithiobacillus ferrooxidans*†

Xiaoqing Meng,[a] Su Yan,[a] Wenzhu Wu,[c] Guanyu Zheng *[ab] and Lixiang Zhou[ab]

Heterogeneous Fenton-like degradation of phenanthrene in aqueous solution was investigated using schwertmannite biosynthesized by *Acidithiobacillus ferrooxidans* LX5 as a catalyst. The effects of different reaction parameters including catalyst loading, H_2O_2 concentration, initial solution pH and inorganic anions on the Fenton-like degradation of phenanthrene were studied. Results showed that the biosynthesized schwertmannite had an effective catalytic ability on phenanthrene degradation. The degradation efficiency of phenanthrene was 99.0% within 3–5 h reaction under conditions of H_2O_2 200 mg L^{-1}, schwertmannite 1 g L^{-1}, phenanthrene 1 mg L^{-1} and pH 3.0–4.5. The degradation was mainly *via* a surface mechanism, in which phenanthrene was readily adsorbed on the surface of schwertmannite and then oxidized by $^{\cdot}OH$ produced from H_2O_2 decomposition. The XPS results of schwertmannite before and after Fenton-like degradation of phenanthrene revealed the change of Fe^{2+}/Fe^{3+} species on the surface of schwertmannite. Moreover, phthalates, octadecanoic acid and 9,10-phenanthraquinone were identified by GC-MS analyses as the main intermediate compounds during phenanthrene degradation, and all the intermediates were finally mineralized. The repeated use of biosynthesized schwertmannite for phenanthrene degradation illustrated its stability and reusability as a Fenton-like catalyst. Therefore, schwertmannite biosynthesized using *A. ferrooxidans* is an excellent catalyst for the degradation of phenanthrene in heterogeneous Fenton-like reactions.

Received 6th March 2017
Accepted 8th April 2017

DOI: 10.1039/c7ra02713c

rsc.li/rsc-advances

1. Introduction

Polycyclic aromatic hydrocarbons (PAHs), organic compounds consisting of at least two fused benzene rings, are highly toxic, carcinogenic and resistant to natural degradation, subsequently causing a serious threat to human health through the food chain.[1–3] The European Community and the U.S. Environmental Protection Agency have listed them as priority pollutants. Wastewater contaminated with PAHs is usually enriched at the sites of manufactured gas plants, refineries and many other chemical industries.[4,5] Owing to their strong persistence and ubiquitous occurrence, substantial studies have been devoted to seek a highly efficient treatment to remove PAHs from industrial wastewater.

Advanced oxidation processes (AOPs) including Fenton-catalysis, photo-catalysis and ozonation have become important technologies for the degradation of persistent organic pollutants (POPs). Among the AOPs, Fenton treatment shows great oxidative potential,[6,7] which is based on the catalyzed decomposition of hydrogen peroxide (H_2O_2) by ferrous ion to generate the strong oxidant hydroxyl radicals. Conventional Fenton treatment is frequently limited by the required optimal pH of around 3.0 to prevent the precipitation of ferrous ion, and the treatment process would produce a large amount of ferric hydroxide sludge during the neutralization stage.[8,9] Moreover, the oxidation efficiency of Fenton process can be significantly decreased by the presence of various inorganic anions, consequently limiting its usage in the treatment of high salinity wastewater.[10,11] Thus, heterogeneous Fenton-like oxidation is developed to overcome the limitations associated with conventional Fenton treatment.[12,13]

Heterogeneous Fenton-like oxidation is initiated by hydrogen peroxide, and hydroxyl radicals can be produced on the surface of the catalysts or in bulk solution.[13,14] Over the last two decades, heterogeneous Fenton-like oxidation catalyzed by goethite, magnetite, ferrihydrite or limonite, *etc.*, has been used to treat water or soils contaminated by organic pollutants.[9]

[a]*Department of Environmental Engineering, College of Resources and Environmental Sciences, Nanjing Agricultural University, Nanjing 210095, China. E-mail: gyzheng@njau.edu.cn; Fax: +86 25 84395160; Tel: +86 25 84395160*

[b]*Jiangsu Collaborative Innovation Center for Solid Organic Waste Resource Utilization, Nanjing 210095, China*

[c]*Nanjing Institute of Environmental Science, Ministry of Environmental Protection of PRC, Nanjing 210042, China*

† Electronic supplementary information (ESI) available. See DOI: 10.1039/c7ra02713c

Pinto *et al.*[15] showed that the oxidation of methylene blue was caused by hydroxyl radicals produced on the surface of δ-FeOOH, and the contribution of soluble Fe on methylene degradation was negligible. Xue *et al.*[16] revealed that the Fenton-like oxidation of pentachlorophenol (PCP) catalyzed by magnetite was dominated by the reactions on the catalyst surface, and in details PCP was readily adsorbed on a fixed number of surface active sites and then attacked by hydroxyl radicals produced from the decomposition of H_2O_2. Toda *et al.*[17] used sulfurized limonite as a catalyst to decompose methylene blue and found that $^{\bullet}OH$ was formed by a heterogeneous reaction on the surface of sulfurized limonite and a Fenton reaction catalyzed by dissolved ferrous ion.

Schwertmannite is a Fe(III)-hydroxysulfate with poorly crystalline structure and high surface area, which is abundant in nature because of its extensive presence in iron- and sulfate-rich mine drainage[18,19] or sludge bioleaching environment.[20] The chemical formula of schwertmannite is $Fe_8O_8(OH)_{8-2x}(SO_4)_x$, $(1 \leq x \leq 1.75)$,[21] and its unit cell always consists of eight $FeO_3(OH)_3$ octahedra forming double chains which are shared over edges and run parallel to the *b*-axis.[22] Schwertmannite can be synthesized through either chemical methods, including a dialysis technique[18,23,24] and a chemically oxidative synthesis method,[23–25] or a biological method using iron-oxidizing bacterium *Acidithiobacillus ferrooxidans*. The dialysis technique usually needs a dialysis period of more than 30 days,[18,23,24] which is time-consuming and inefficient for schwertmannite synthesis.[20] The chemically oxidative synthesis of schwertmannite through adding H_2O_2 into $FeSO_4$ solution takes one to several days to complete, and the specific surface areas of the produced schwertmannite are 4–14 m^2 g or 2.06–16.30 m^2 g.[23,25] Recently, the biological synthesis of schwertmannite receives much more attention, because schwertmannite can be biosynthesized by *A. ferrooxidans* within only 2–3 days and the specific surface areas of the produced schwertmannite are much larger than that synthesized using chemically oxidative synthesis method.[24,26] For instances, Li *et al.*[26] reported that the specific surface area of biosynthesized schwertmannite using *A. ferrooxidans* was 45.63 m^2 g^{-1}, larger than 3.17 m^2 g^{-1} of chemically synthesized samples. In addition, Li *et al.*[26] and Liu *et al.*[25] found that the schwertmannite yield of biological method is comparatively or much higher than that of chemically oxidative synthesis method. Therefore, the biosynthesis method using *A. ferrooxidans* is a more attractive approach over chemical methods for schwertmannite production, in terms of the specific surface area and synthesis yield of produced schwertmannite.

Recently, some studies attempted to use chemosynthetic schwertmannite as a catalyst in the heterogeneous Fenton-like oxidation to oxidize nitrobenzene and phenol.[27,28] However, the catalytic capacity of biosynthetic schwertmannite and the associated mechanism are still unclear in the heterogeneous Fenton-like oxidation of hydrophobic organic pollutants. Especially, previous studies reported that the catalysts with much larger specific surface areas usually would have much higher catalytic activities, because of their large numbers of active sites for H_2O_2 decomposition.[29] Therefore, the objectives of the present study are to (1) investigate the effect of reaction conditions including the loading of biosynthetic schwertmannite, concentration of H_2O_2, solution initial pH, and the presence of inorganic anions on the degradation of phenanthrene catalyzed by biosynthetic schwertmannite and H_2O_2, (2) reveal the associated catalytic degradation mechanism and possible transformation pathway of phenanthrene in biosynthetic schwertmannite/H_2O_2 system, and (3) study the stability of biosynthetic schwertmannite during its repeated use in the catalytic degradation of phenanthrene.

2. Materials and methods

2.1. Reagents

Phenanthrene (≥99%) was purchased from Aladdin Co., Ltd. Acetonitrile, methanol and *n*-hexane were purchased from Sigma Aldrich Co. Ltd at HPLC grade, and dichloromethane and acetone were supplied by Aladdin Co., Ltd at HPLC grade. Hydrogen peroxide (30% solution) and other reagents were obtained from Sinopharm Chemical Regent Beijing Co., Ltd and used as received. All solutions and suspensions were prepared by using deionized water.

2.2. Preparation of catalysts

Biosynthetic schwertmannite was prepared in the laboratory according to the method described in previous studies.[20] Briefly, 20 mL of freshly prepared *A. ferrooxidans* LX5 cell suspensions with a cell density of 3×10^8 cells per mL were introduced into 1000 mL Erlenmeyer flask containing 480 mL of ferrous sulfate solution with ferrous ion concentration of 0.144 M. The flasks were then incubated for 2 days at 180 rpm and 28 °C in a rotary shaker. The precipitates formed in the flasks were harvested by filtering through a Whatman no. 4 filter paper, sequentially washed with acidified water with pH 2.0 and deionized water for three times to remove soluble impurities, and dried at 50 °C to a constant weight. The preparation of chemosynthetic schwertmannite and chemosynthetic goethite followed the methods of Liu *et al.*[25] and Manning *et al.*[30] The detailed procedures can be found in the ESI.†

2.3. Characterization of catalysts

The morphology of biosynthetic schwertmannite was examined by scanning electron microscope (SEM, Hitachi S-4700) at 20 kV accelerating voltage. The crystal structure of biosynthetic schwertmannite was determined by X-ray powder diffraction (XRD, ThermoFisher XTRA) using an X-ray diffractometer fitted with Cu Kα radiation (40 kV and 40 mA), and samples were scanned from $2\theta = 10°$–$70°$ with a $2\theta = 0.02°$ step-size. The functional groups of biosynthetic schwertmannite were determined by Fourier transform infrared spectroscopy (FTIR) with a wavelength range of 400–4000 cm^{-1}, which was scanned 32 times and resolution ratio of 0.09 cm^{-1}. The specific surface area of biosynthetic schwertmannite was measured by using the Brunauer–Emmett–Teller (BET) through N_2 adsorption–desorption method (BET, Tristar 3000, Micromeritics).

2.4. Catalytic degradation of phenanthrene

To prepare 1 mg L^{-1} phenanthrene solution, phenanthrene was firstly dissolved in acetone to make a solution with a concentration of 1000 mg L^{-1}, and then 1 mL prepared solution was diluted to a concentration of 1 mg L^{-1} using deionized water.[31]

The phenanthrene degradation experiments were conducted in 35 mL glass vessels with screw caps having a PTFE-lined septum. In each vessel, the reaction medium was prepared by adding a certain amount of schwertmannite to 10 mL phenanthrene solution with a concentration of 1 mg L^{-1}, and the solution initial pH was adjusted to defined values using 1 M $HClO_4$ or 1 M NaOH.[32] The reaction was then initiated by adding a certain amount of H_2O_2 into the glass vessels. All experiments were carried out under dark conditions and shaken in a rotary shaker at 180 rpm and 28 °C. At the given reaction time intervals, vessels were taken out and added with 3 mL methanol to quench the reaction. Vessels taken out were added with ten drops of 1 M H_2SO_4 to totally dissolve schwertmannite. Phenanthrene in the resulting solution was extracted using dichloromethane for quantitative analysis of phenanthrene degradation efficiency using a high performance liquid chromatography (HPLC), and alternatively it was extracted using *n*-hexane to indentify the intermediate products during the phenanthrene degradation using a gas chromatography mass spectrometer (GC-MS). Meanwhile, parallel samples in withdrawn vessels were filtered through a 0.22 μm glass fiber filter paper, and the obtained supernatant was used for the determination of the concentrations of total Fe, Fe^{2+} and Fe^{3+}, H_2O_2 concentration and total organic carbon (TOC) content. To determine the removal efficiency of phenanthrene from the solution, the supernatant was directly extracted using dichloromethane and quantified using HPLC, which is without the procedure of dissolving schwertmannite. Initial loading content of schwertmannite was changed from 0.1 to 2 g L^{-1} to test the loading of catalyst on the catalytic degradation efficiency of phenanthrene. To verify the presence of $^{\cdot}OH$ in the degradation system, methanol was used as a scavenger to give a volume percentage ranging from 1% to 10%,[27,28] which was added before adding H_2O_2 to the solution. Under the optimum reaction condition, the schwertmannite was collected at the end of the experiment, washed with the deionized water, and dried to a constant weight. The oxidation states of iron species on the schwertmannite surface was measured by the X-ray photoelectron spectrum (XPS), which was performed in a Kratos AXIS His, mono Al Kα system (Energy 1486.7 eV, Kratos Analytical, Japan).

To explore the presence of inorganic anions on the effect of phenanthrene degradation, SO_4^{2-}, $H_2PO_4^-$, NO_3^- and Cl^- with the respective concentration ranging from 50 to 200 mg L^{-1} were introduced to the degradation system which contained 1 mg L^{-1} phenanthrene, 1 g L^{-1} schwertmannite and 200 mg L^{-1} H_2O_2, at pH 3.0. The stability and reusability of schwertmannite was also investigated in a multi-cycle experiment. In each cycle, the initial concentrations of phenanthrene, H_2O_2 and schwertmannite were 1 mg L^{-1}, 200 mg L^{-1} and 1 g L^{-1}, respectively, and the reaction time and solution initial pH were 12 h and 3.0. The used catalyst was collected at the end of each oxidation experiment, washed with the deionized water, dried enough, and then used in the next cycle experiment. In each cycle experiment, the degradation efficiency of phenanthrene and TFe concentration in the solution were measured. Biosynthetic schwertmannite was characterized by using X-ray powder diffraction (XRD) and Fourier transform infrared spectroscopy (FTIR) after 12 times of repeated use.

2.5. Analytical methods

The concentration of phenanthrene was analyzed using a HPLC (HPLC-1260, Agilent) equipped with UV detection wavelength of 254 nm. Waters PAH C_{18} column (5 μm, 4.6 mm × 250 mm) was used for the separation of phenanthrene. Samples were injected at 20 μL at a column temperature of 27 °C, and the mobile phase was the mixture of water (40%) and acetonitrile (60%). Phenanthrene and its intermediate products were identified using a SHIMADZU gas chromatograph (GC-2010) incorporated with a mass spectrometer operated on a full scan mode (50–550 amu), where the MS capillary column (250 μm, 0.25 μm × 30 m) was used. Helium was used as carrier gas at a flow rate of 1.0 mL min^{-1}. The initial oven temperature was 80 °C (5 min holding) and continued to rise temperature to 300 °C at a speed of 10 °C min^{-1} (10 min holding). The concentration of dissolved Fe was determined by using Inductively Coupled Plasma (ICP, Agilent 5100). The concentration of H_2O_2 and the content of total organic carbon were measured using the titanium sulfate method and TOC analyzer (TOC-5000, Shimadzu), respectively.

3. Results and discussion

3.1. Characterization of biosynthetic schwertmannite and its catalytic capability

Oxidation of ferrous sulfate by *A. ferrooxidans* LX5 cell suspensions resulted in the formation of iron precipitates. The iron precipitates formed were visualized by SEM. As shown in Fig. 1a and b, they were consisted of aggregates of spherical particles, and the surface of spherical particles showed a "hedge-hog" morphology which is typical for schwertmannite.[19] The XRD patterns of iron precipitates (Fig. 1c) displayed a weak crystalline structure with seven typical broad characteristic peaks (2θ: 18.24, 26.27, 35.16, 39.49, 46.53, 55.29, 61.34°), and all diffraction peaks well matched those of the standard diffraction data for schwertmannite (JCPDS no. 47-1775), suggesting that the iron precipitates formed are pure schwertmannite particles. The BET analysis revealed that the specific surface area of the biosynthesized schwertmannite was 54.5 m^2 g^{-1}.

The degradation of 1 mg L^{-1} phenanthrene catalyzed by biosynthetic schwertmannite, chemosynthetic schwertmannite and chemosynthetic goethite was evaluated under the same experimental conditions of 1.0 g L^{-1} catalyst, and 200 mg L^{-1} H_2O_2 at pH 3.0, and results are shown in Fig. 2. It can be found that as high as 99% of phenanthrene degradation was achieved within only 3 h in Fenton-like reaction catalyzed by biosynthetic schwertmannite. However, within the same reaction period (3 h), less than 28.6% and 45.4% of phenanthrene was degraded in Fenton-like reaction catalyzed by chemosynthetic schwertmannite

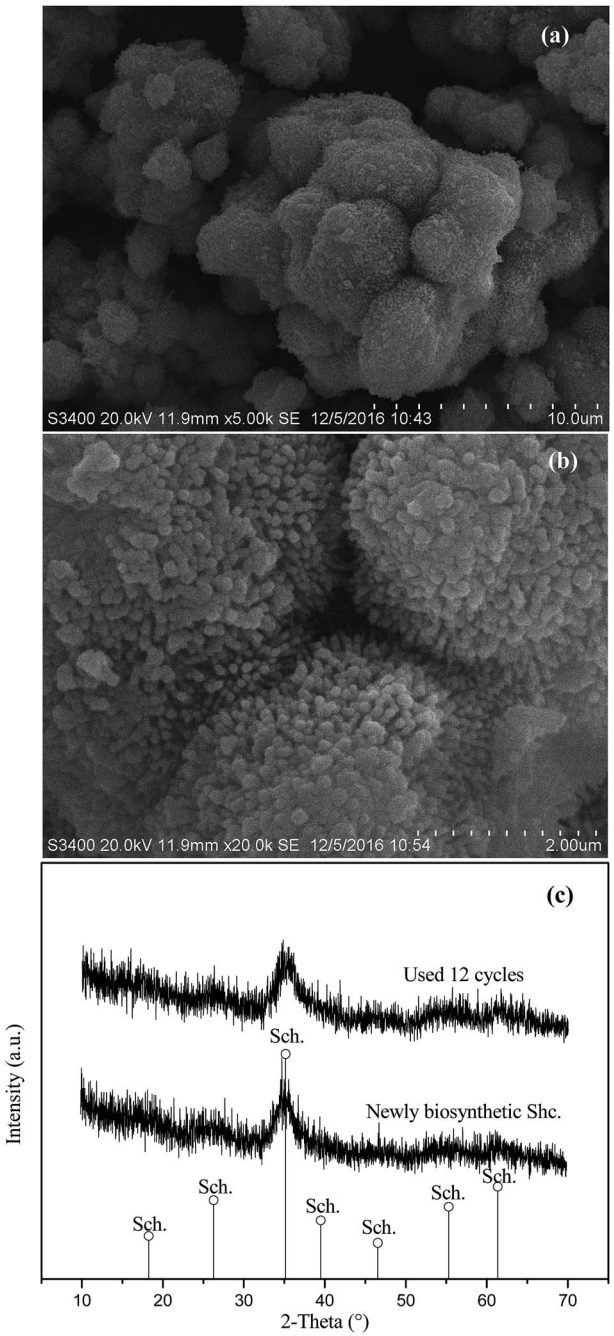

Fig. 1 SEM images of the biosynthetic schwertmannite particles: ×2000 (a) and ×20 000 (b), and XRD (c) analyses of newly biosynthesized schwertmannite and the schwertmannite after being used for 12 cycles. Experimental conditions were $[\text{phenanthrene}]_0 = 1$ mg L^{-1}, $[\text{schwertmannite}]_0 = 1$ g L^{-1}, $[H_2O_2]_0 = 200$ mg L^{-1}, solution initial pH = 3.0, and reaction time of 12 h in each cycle.

and chemosynthetic goethite, respectively. These results clearly indicated that the catalytic activity of biosynthetic schwertmannite in Fenton-like system was much higher than that of either chemosynthetic schwertmannite or chemosynthetic goethite. The much poorer performance of chemosynthetic schwertmannite in the catalytic degradation of phenanthrene may be related to its relatively low specific surface area (6.84 $m^2 g^{-1}$), because of lack of

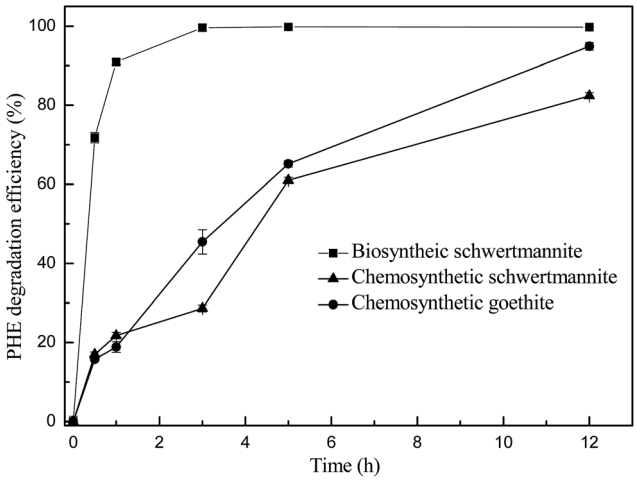

Fig. 2 The degradation of phenanthrene catalyzed by biosynthetic schwertmannite, chemosynthetic schwertmannite and chemosynthetic goethite with working volume of 10 mL. Experimental conditions were $[\text{phenanthrene}]_0 = 1$ mg L^{-1}, $[H_2O_2]_0 = 200$ mg L^{-1}, and solution initial pH = 3.0.

"hedge-hog" morphology on its particle surfaces (as shown in Fig. S1†), and the discrepancy of catalytic capabilities between biosynthetic schwertmannite and goethite probably resulted from much less surface active sites of goethite.[29,33,34]

3.2. Effect of schwertmannite loading, H_2O_2 concentration, and solution initial pH on the degradation of phenanthrene

The effect of biosynthetic schwertmannite loading on the catalytic degradation of phenanthrene is shown in Fig. 3a. The loading of 0.1 g L^{-1} biosynthetic schwertmannite only resulted in 57.3% degradation of 1 mg L^{-1} phenanthrene within 12 h of reaction, and 12 h was consumed to degrade 98.3% of phenanthrene when the loading of biosynthetic schwertmannite was 0.5 g L^{-1}. However, phenanthrene was totally degraded within only 3–5 h at the schwertmannite loading of 1 g L^{-1}, and the degradation of phenanthrene was not further improved when the loading of biosynthetic schwertmannite was increased to 2.0 g L^{-1}. Thus, 1.0 g L^{-1} of schwertmannite loading is suitable for the degradation of phenanthrene in the Fenton-like reaction catalyzed by biosynthetic schwertmannite.

The concentration of H_2O_2 is an important factor influencing the Fenton or Fenton-like reaction, since it directly relates to the amount of hydroxyl radicals produced in the catalytic reactions.[29] The effect of H_2O_2 concentration on the degradation of phenanthrene by Fenton-like reaction catalyzed by biosynthetic schwertmannite was investigated by changing H_2O_2 concentration from 16.7 to 500 mg L^{-1} at pH 3.0, with the schwertmannite loading of 1 g L^{-1} and phenanthrene concentration of 1 mg L^{-1}. As shown in Fig. 3b, the degradation efficiency of phenanthrene within 5 h of Fenton-like reaction catalyzed by biosynthetic schwertmannite was enhanced from 25.7% to 99.9% when increasing H_2O_2 concentration from 16.7 to 200 mg L^{-1}. Actually, when the concentration of H_2O_2 was 200 mg L^{-1}, about 99.6% of phenanthrene can be degraded in

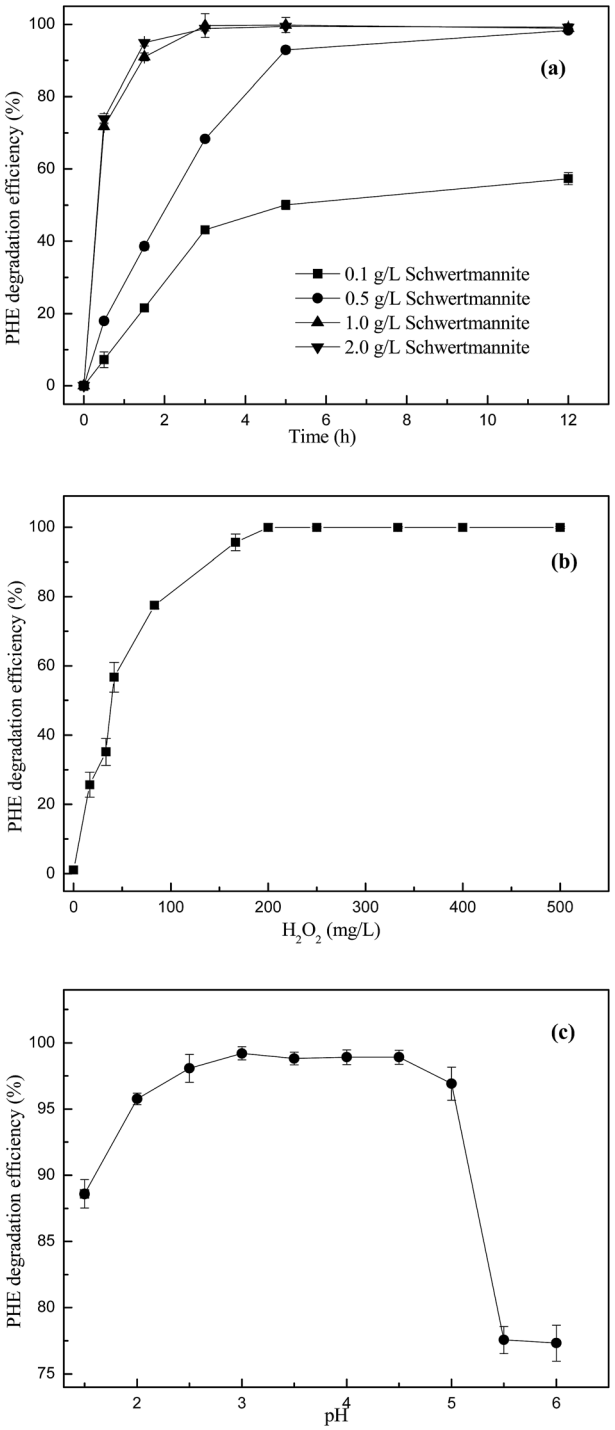

Fig. 3 Effect of schwertmannite loading (a), H_2O_2 concentration (b) and solution initial pH (c) on the degradation of phenanthrene with working volume of 10 mL. Experimental conditions of schwertmannite loading were $[phenanthrene]_0 = 1$ mg L^{-1}, $[H_2O_2]_0 = 200$ mg L^{-1}, and solution initial pH = 3.0; experimental conditions of H_2O_2 concentration were $[phenanthrene]_0 = 1$ mg L^{-1}, $[schwertmannite]_0 = 1$ g L^{-1}, solution initial pH = 3.0 and reaction time of 5 h; experimental conditions of solution initial pH were $[phenanthrene]_0 = 1$ mg L^{-1}, $[schwertmannite]_0 = 1$ g L^{-1}, $[H_2O_2]_0 = 200$ mg L^{-1} and reaction time of 5 h.

only 3 h of reaction (Fig. 3a). Previous studies found that higher concentration of H_2O_2 may scavenge the produced reactive oxidation species (like $^{\bullet}OH$) to form $HO_2^{\bullet}$, thus lowering the degradation efficiency of organics, because the oxidation potential of $HO_2^{\bullet}$ was much lower than that of $^{\bullet}OH$.[27] However, the degradation of phenanthrene was not lowered when further increasing H_2O_2 concentration beyond 200 mg L^{-1}. Since too much H_2O_2 would definitely raise the cost of treatment, the optimum H_2O_2 concentration was 200 mg L^{-1} for the efficient degradation of 1 mg L^{-1} phenanthrene within 3–5 h of reaction catalyzed by biosynthetic schwertmannite.

Many studies reported that the initial pH of solution seriously affects the performance of the Fenton-like process in degrading pollutants, because of the role of solution pH in controlling the catalytic activity and the hydrogen peroxide stability.[35–37] In addition, an acidic condition is usually beneficial for the degradation of organics in Fenton-like reactions catalyzed by iron oxide minerals including magnetite, hematite and goethite because the dissolution of iron oxide minerals can easily occur at acidic conditions to release dissolve iron to catalyze homogenous Fenton-like reactions.[29] The effect of solution initial pH on the degradation of phenanthrene was determined within a pH range of 1.5–6.0. As shown in Fig. 3c, the degradation efficiency of phenanthrene was enhanced from 88.6% to 99.2% when increasing the solution initial pH from 1.5 to 3.0. Obviously, the maximum degradation efficiency of phenanthrene was achieved in the solution initial pH range of 3.0–4.5, which was higher than 99.0%. When the solution initial pH was higher than 4.5, the degradation of phenanthrene decreased rapidly. Especially, the degradation efficiency of phenanthrene was only 77.6% when the solution initial pH was 5.5. Therefore, the optimum pH for the degradation of phenanthrene catalyzed biosynthetic schwertmannite is 3.0–4.5, at which pH values more than 99.0% of 1 mg L^{-1} phenanthrene can be degraded effectively.

3.3. Mechanism of phenanthrene degradation

In order to verify the presence of $^{\bullet}OH$ in the Fenton-like reaction catalyzed by biosynthetic schwertmannite, methanol was chosen as a $^{\bullet}OH$ scavenger during the catalytic degradation of phenanthrene. It can be seen from Fig. 4 that the degradation of phenanthrene was rapidly lowered by the presence of methanol in the system. Only 64.3% and 30.4% of phenanthrene was degraded within 12 h of reaction when 1% or 5% of methanol was added, respectively. In addition, the degradation of phenanthrene was totally inhibited by the presence of 10% methanol. These results clearly indicated that phenanthrene was catalytically degraded by $^{\bullet}OH$ generated by H_2O_2 decomposition in the Fenton-like reaction catalyzed by biosynthetic schwertmannite.[15,28] To further reveal the mechanism responsible for phenanthrene degradation, dissolved iron concentration, H_2O_2 concentration and TOC content in the solution were monitored during the degradation of 1 mg L^{-1} phenanthrene catalyzed by 1 g L^{-1} of schwertmannite and 200 mg L^{-1} H_2O_2 at pH 3.0. As shown in Fig. 5a, the ferrous concentration reached a peak value of 0.70 mg L^{-1} at 5 h when phenanthrene was completely

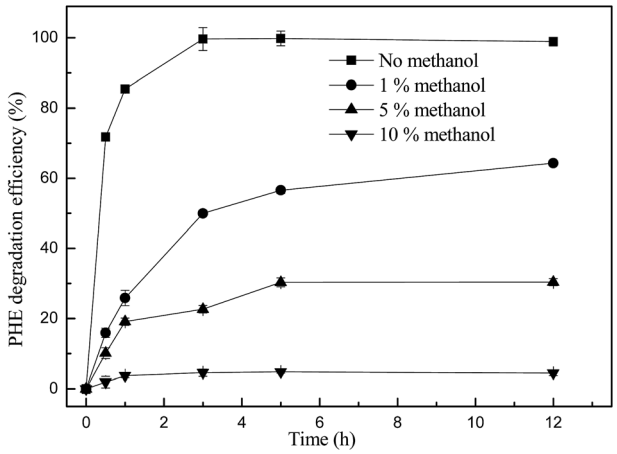

Fig. 4 Effect of methanol addition on the degradation of phenanthrene with working volume of 10 mL. Experimental conditions were $[phenanthrene]_0 = 1$ mg L^{-1}, $[schwertmannite]_0 = 1$ g L^{-1}, $[H_2O_2]_0 = 200$ mg L^{-1}, and solution initial pH = 3.0.

degraded, and then its concentration decreased to 0.28 mg L^{-1} at 60 h of reaction, which could be ascribed to the oxidation of ferrous ions into ferric ions by remaining $^{\bullet}OH$ and H_2O_2 in the solution. After 8 h of reaction, the concentrations of ferric and total dissolved iron attained 2.17 and 2.70 mg L^{-1}, respectively, which suggests that Fe inside the structure of schwertmannite or adsorbed on the surface of schwertmannite were released into the solution during the reaction. Furthermore, about 3.03 mg L^{-1} of iron dissolved into solution after 60 h of reaction, only equivalently 0.68% of total iron of 1.0 g L^{-1} catalyst used, which shows a very slow leaching of iron from biosynthetic schwertmannite. As shown in Fig. 5b, the TOC content decreased sharply from 0.94 mg L^{-1} to an undetectable level within the first 5 h of reaction, which clearly illuminated that 1 mg L^{-1} of phenanthrene was completely mineralized by the reaction catalyzed by schwertmannite and H_2O_2. Correspondingly, the concentration of H_2O_2 also declined from 200 to 163.6 mg L^{-1} within the first 5 h of reaction, and then the excessive H_2O_2 was run out gradually.

To clarify the contribution of homogenous Fenton reaction catalyzed by dissolved ferric ion on the degradation of phenanthrene, the highest dissolved ferric ion concentration during the degradation of 1 mg L^{-1} phenanthrene catalyzed by 1 g L^{-1} of schwertmannite and 200 mg L^{-1} H_2O_2 at pH 3.0, 2.76 mg L^{-1} of ferric ion, was used to catalyze a homogenous Fenton reaction to degrade phenanthrene. As shown in Fig. 6, only 39.8% of phenanthrene could be degraded by the homogenous Fenton reaction catalyzed by 2.76 mg L^{-1} of dissolved ferric ion and 200 mg L^{-1} H_2O_2 at pH 3.0 after 5 h, but as high as 100% of phenanthrene was degraded in 5 h by the reaction catalyzed by 1 g L^{-1} schwertmannite and 200 mg L^{-1} H_2O_2 at pH 3.0. It should be taking into account that 2.76 mg L^{-1} Fe^{3+} was not available from the beginning of the Fenton-like reaction catalyzed by schwertmannite, and thus the degradation of phenanthrene by the homogenous Fenton reaction should be much lower than 39.8%. This result clearly indicated that the degradation of phenanthrene did not merely result from the homogenous Fenton

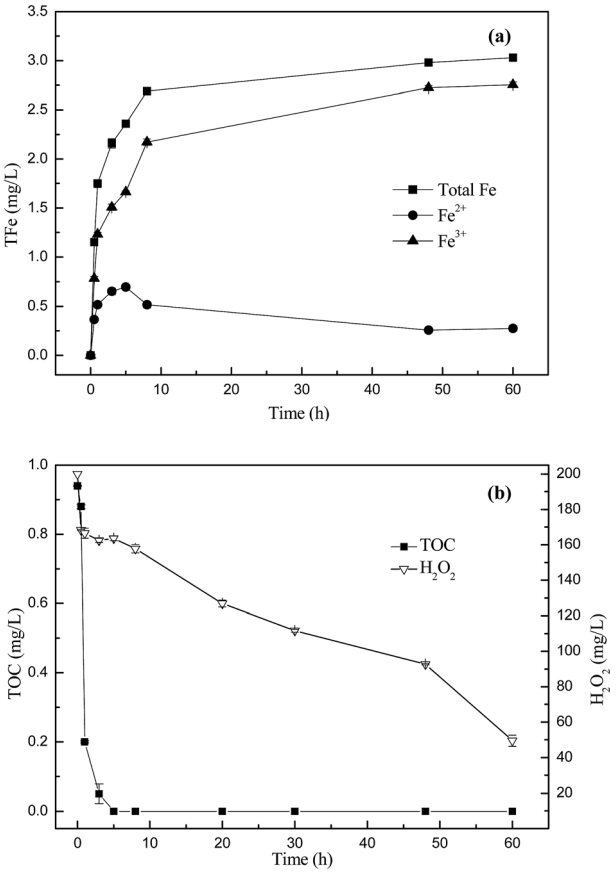

Fig. 5 Changes of total Fe (TFe), Fe^{2+} and Fe^{3+} concentration (a), H_2O_2 concentration and TOC content (b) in the solution during the degradation of 1 mg L^{-1} phenanthrene catalyzed by 1 g L^{-1} of schwertmannite and 200 mg L^{-1} H_2O_2 at pH 3.0.

reaction catalyzed by dissolved ferric ion, and both homogenous Fenton reaction catalyzed by dissolved ferric ion and heterogeneous Fenton-like reaction catalyzed schwertmannite played

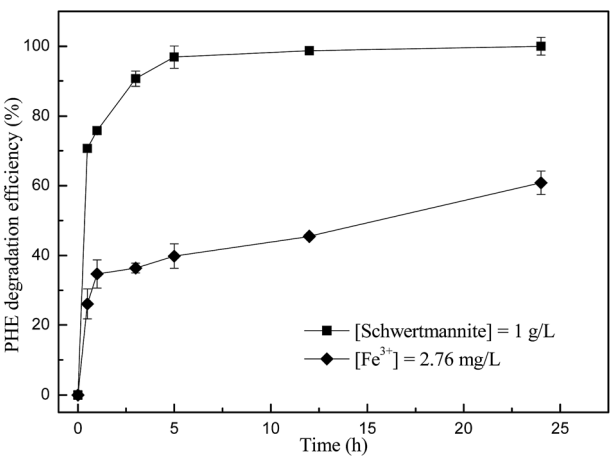

Fig. 6 Change of phenanthrene degradation efficiency during the degradation catalyzed by 1 g L^{-1} schwertmannite or 2.7 mg L^{-1} Fe^{3+}, with working volume of 10 mL. Experimental conditions: $[phenanthrene]_0 = 1$ mg L^{-1}, $[H_2O_2]_0 = 200$ mg L^{-1}, and solution initial pH = 3.0.

important roles in degrading phenanthrene. In addition, it seems that the heterogeneous Fenton-like reaction catalyzed by schwertmannite was much more effective than the homogenous Fenton reaction catalyzed by dissolved ferric ion in degrading phenanthrene during the degradation of 1 mg L^{-1} of phenanthrene catalyzed by schwertmannite and H_2O_2.

Although phenanthrene could be degraded in only 5 h by the reaction catalyzed by 1 g L^{-1} of schwertmannite and 200 mg L^{-1} H_2O_2 at pH 3.0, its removal from the solution seems much faster. Here, the degradation referred to that phenanthrene in the reaction system was oxidized into small molecular compounds, or even CO_2 and H_2O, while the removal means the disappearance of phenanthrene from the reaction solution through both oxidation and adsorption processes. As shown in Fig. 7, 1 mg L^{-1} of phenanthrene was completely removed from the solution in only 2 hours when the degradation efficiency of phenanthrene was only 55.1%. This result obviously indicated that phenanthrene was readily adsorbed onto the surface of schwertmannite particles probably because of strong sorption capacity of schwertmannite for hydrophobic organic pollutants such as phenanthrene. In fact, adsorption experiments revealed that the sorption capacity of biosynthetic schwertmannite for phenanthrene is as high as 0.74 mg g^{-1} (data not shown). The strong sorption capacity of biosynthetic schwertmannite for phenanthrene clearly indicates that the degradation of phenanthrene by biosynthetic schwertmannite/H_2O_2 reaction was mainly *via* a surface mechanism, in which phenanthrene can be readily adsorbed on the surface of schwertmannite and then oxidized by hydroxyl radical produced from H_2O_2 decomposition.

The XPS results of biosynthetic schwertmannite before and after Fenton-like degradation of phenanthrene are shown in Fig. 8 and Table S1.† The Fe 2p lines are broad and can be deconvoluted into two components with line position at 711.1 and 712.8 eV, respectively. These two components correspond to the Fe^{3+} and Fe^{2+} species.[38] Before the Fenton-like reaction, the major surface iron specie of biosynthetic schwertmannite is found to be Fe^{3+}, which contributes to 58.2% of the total surface iron atoms, and 41.8% of the total iron surface atoms was Fe^{2+}. For biosynthetic schwertmannite after the Fenton-like reaction, the intensity ratio of Fe^{2+}/Fe^{3+} species was changed to 54.5 : 45.5. The curve fitting was carried out using the Gaussian–Lorentzian ratio = 20 (G : L = 20 : 80), the symmetry factor of 0.4, and the χ^2 of 2.05. The binding energy of Fe 2p, and Fe^{2+} and Fe^{3+} surface concentration on the biosynthetic schwertmannite catalyst before and after phenanthrene degradation were listed in Table S1.† The change of Fe^{2+}/Fe^{3+} species on the surface of biosynthetic schwertmannite implies that the biosynthetic schwertmannite take part in oxidation–reduction reaction during phenanthrene degradation and the Fenton-like degradation of phenanthrene mainly occurred on the surface of biosynthetic schwertmannite.

Thus, the Fenton-like degradation of phenanthrene catalyzed by biosynthetic schwertmannite can be explained by the following mechanisms:

$$\equiv Fe^{III} + \text{phenanthrene} \rightarrow \equiv Fe^{III} - \text{phenanthrene} \quad (1)$$

$$\equiv Fe^{III} + H_2O_2 \rightarrow \equiv Fe^{III}H_2O_2 \quad (2)$$

$$\equiv Fe^{III}H_2O_2 \rightarrow \equiv Fe^{II} + {}^{\cdot}HO_2 + H^+ \quad (3)$$

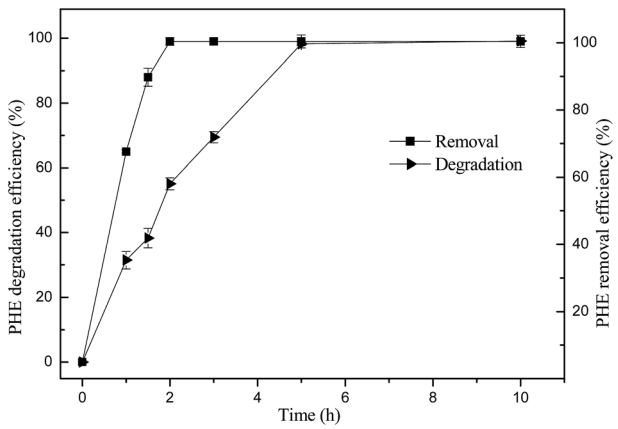

Fig. 7 Changes of phenanthrene degradation efficiency and its removal efficiency during the catalytic degradation with working volume of 10 mL. Experimental conditions were $[\text{phenanthrene}]_0$ = 1 mg L^{-1}, $[\text{schwertmannite}]_0$ = 1 g L^{-1}, $[H_2O_2]_0$ = 200 mg L^{-1}, and solution initial pH = 3.0.

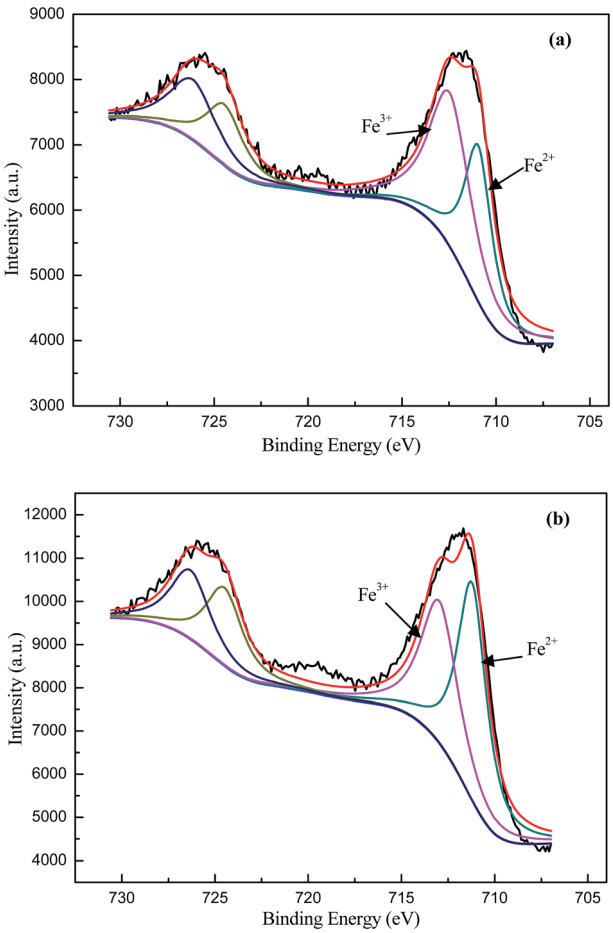

Fig. 8 XPS spectrums of the biosynthetic schwertmannite before (a) and after (b) phenanthrene degradation (Fe 2p line).

$$\equiv Fe^{III} + {}^{\cdot}HO_2 \rightarrow \equiv Fe^{II} + O_2 + H^+ \quad (4)$$

$$\equiv Fe^{II} + H_2O_2 \rightarrow \equiv Fe^{III} + {}^{\cdot}OH + OH^- \quad (5)$$

$$\equiv Fe^{III} - \text{phenanthrene} + {}^{\cdot}OH \rightarrow \equiv Fe^{III} + \text{degradation products} \rightarrow \ldots CO_2 + H_2O \quad (6)$$

At the beginning of Fenton-like degradation of phenanthrene catalyzed by biosynthetic schwertmannite, phenanthrene molecules were readily adsorbed on the surface of schwertmannite to form $\equiv Fe^{III}$ – phenanthrene (eqn (1)), where $\equiv Fe^{III}$ represents Fe^{III} sites on the catalyst surface.[39] The heterogeneous Fenton-like reaction was activated by the formation of a complex between $\equiv Fe^{III}$ and H_2O_2, being assigned as $\equiv Fe^{III}H_2O_2$ (eqn (2)). Then the generated $\equiv Fe^{III}H_2O_2$ species are converted to $\equiv Fe^{II}$ species and ${}^{\cdot}HO_2$ (eqn (3)), and the generated ${}^{\cdot}HO_2$ may further react with $\equiv Fe^{III}$ to produce $\equiv Fe^{II}$ species (eqn (4)). The above formed $\equiv Fe^{II}$ (eqn (3) and (4)) can react with H_2O_2 to generate ${}^{\cdot}OH$ radicals (eqn (5)). The ${}^{\cdot}OH$ radicals thus attack the phenanthrene molecules adsorbed on the surface of schwertmannite and realize the degradation and/or mineralization (eqn (6)). This mechanism is analogous to previous studies on the heterogeneous Fenton-like reactions of the iron-oxide/H_2O_2 system.[29,38]

3.4. Transformation pathway of phenanthrene

The intermediates of phenanthrene degradation were identified by using GC-MS to further reveal its transformation pathway in the Fenton-like reaction catalyzed by biosynthetic schwertmannite. As shown in Fig. S2,† some intermediates were found in the sample with 1 h reaction time, and the characteristics peaks were summarized in Table 1.

According to the standard spectra from the NIST library database, the peak B and E can be assigned to the compound of octadecanoic acid. Correspondingly, the peak C can be assigned to 9,10-phenanthraquinone, and the peak D, F (F1, F2 and F3) and G (G1 and G2) were assigned to the compound phthalate by analyzing the fragmentation pattern of mass spectra, which was not observed before reaction. It was noted that peak G (G1 and G2) was identified as nonyl octyl phthalate, which gives the maximum m/z value of 405 (Fig. S3†). The above stated intermediates are consistent with the previous reports.[40,41] However, no products appeared in the sample with 5 h reaction time, which clearly indicates that all intermediates were finally mineralized into CO_2 and H_2O, consistent with the result of TOC removal.

The above mentioned products were only portion of the reaction intermediates, since some intermediates had too short lifetime and could not be detected by using the current GC-MS analysis. Considering the above products identified and some reported phenanthrene transformation pathways,[41,42] the transformation pathway of phenanthrene in the biosynthetic schwertmannite/H_2O_2 system was temporarily proposed in Fig. 9. In the main, hydroxyl radicals and singlet oxygen attacked the benzene rings of phenanthrene at positions 9 and 10 to ketonize phenanthrene, leading to substituted products such as 9,10-phenanthraquinone (product C).[43] Subsequently, the benzene rings of 9,10-phenanthraquinone can be cleaved and then formed compounds of phthalate. The above phthalate is esterified into dioctyl phthalate (product F1, F2 and F3) and nonyl octyl phthalate (product G1 and G2) in OH-induced oxidation process.[41,44] Afterward, the rest benzene ring is further cleaved, and the formed products can be attacked by hydroxyl radicals continuously until complete mineralization.

Table 1 Identification of intermediates produced during phenanthrene degradation after 1 h reaction time based on GC-MS measurements

Peak	Retention time	m/z	Empirical formula	Compound
A	18.120	178	$C_{14}H_{10}$	Phenanthrene
B	19.717	281	$C_{18}H_{32}O_2$	Octadecanoic acid
C	20.842	208	$C_{14}H_8O_2$	9,10-Phenanthraquinone
D	22.300	390	$C_{24}H_{38}O_4$	Dioctyl phthalate
E	22.742	281	$C_{18}H_{32}O_2$	Octadecanoic acid
F1	24.542	390	$C_{24}H_{38}O_4$	Dioctyl phthalate
F2	24.810	390		
F3	25.085	390		
G1	26.192	405	$C_{25}H_{40}O_4$	Nonyl octyl phthalate
G2	26.342	405		

3.5. Effects of inorganic anions on the degradation of phenanthrene and the stability and reusability of biosynthetic schwertmannite

Inorganic anions were always detected in industrial wastewater or underground water, and their existences usually affect the oxidation efficiency of Fenton process.[45–47] In the present study, the concentrations of inorganic anions were controlled in a range of 50–200 mg L^{-1} and the phenanthrene degradation experiments were carried out in 5 h. The experimental results were shown in Fig. 10, and it could be found that the inhibitory effect of SO_4^{2-}, $H_2PO_4^-$, NO_3^- or Cl^- on the degradation of phenanthrene was enhanced with the increase of their respective concentration from 50 to 200 mg L^{-1}. However, these inorganic anions presented different potential in respect of inhibiting the degradation of phenanthrene, and the inorganic anions studied suppressed the degradation of phenanthrene in a sequence of $SO_4^{2-} > H_2PO_4^- > NO_3^- > Cl^-$. After 5 h reaction, the efficiency of phenanthrene degradation was only 63.74%, 71.67%, 72.71% and 77.24% in the presence of 200 mg L^{-1} of SO_4^{2-}, $H_2PO_4^-$, NO_3^- and Cl^-, respectively. Actually, previous studies reported that SO_4^{2-} and $H_2PO_4^-$ could easily combine with ferric ion on the surface of iron oxides, and formed sulfate–ferric or phosphoric–ferric complexes, resulting in a very slow decomposition of H_2O_2.[10] Liu *et al.*[47] showed that both SO_4^{2-} and Cl^- had a potential of scavenging hydroxyl radicals and would form $SO_4^{\cdot-}$ (2.43 V), $Cl^{\cdot}$ (2.41 V) and $Cl_2^{\cdot-}$ (2.09 V) at pH 3.0, which had lower oxidation ability than hydroxyl radicals. Besides, Cl^- could interact with the iron oxide surface through specific adsorption,[48] and NO_3^- may also have the ability to scavenge ${}^{\cdot}OH$ to lower the degradation efficiency of organics.[28]

From the view of application, the long-term stability of biosynthetic schwertmannite should also be considered, and thus

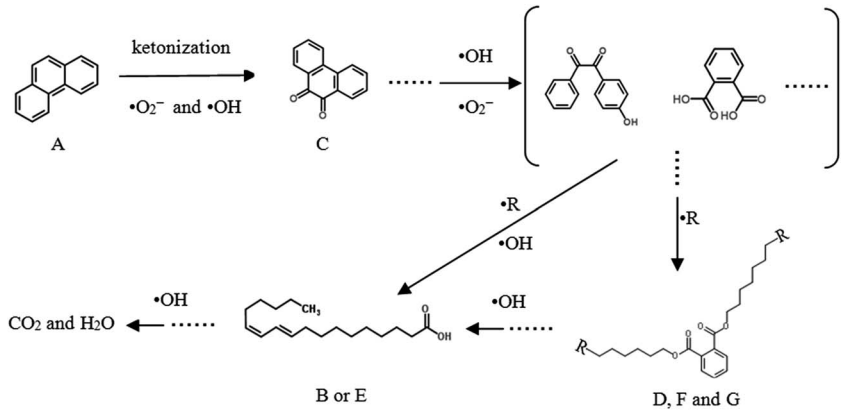

Fig. 9 Proposed transformation pathway of phenanthrene catalyzed by biosynthetic schwertmannite/H_2O_2 reaction.

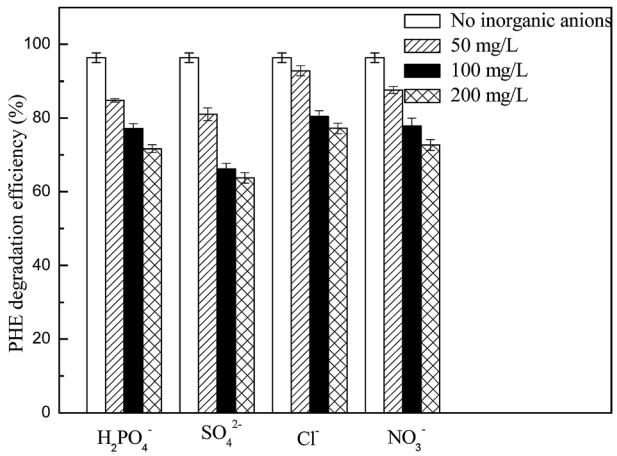

Fig. 10 Effect of inorganic anions ($H_2PO_4^-$, SO_4^{2-}, Cl^-, NO_3^-) on the degradation of phenanthrene with working volume of 10 mL. Experimental conditions were $[phenanthrene]_0 = 1$ mg L^{-1}, $[schwertmannite]_0 = 1$ g L^{-1}, $[H_2O_2]_0 = 200$ mg L^{-1}, and solution initial pH = 3.0.

its catalytic capacity and the leaching of Fe from schwertmannite were investigated in a multi-cycle experiment. In each cycle, the initial concentrations of phenanthrene, H_2O_2 and schwertmannite were 1 mg L^{-1}, 200 mg L^{-1} and 1 g L^{-1}, respectively, and the reaction time and solution initial pH were 12 h and 3.0. As shown in Fig. 11a, the degradation efficiency of phenanthrene decreased from 99.0% to 80.0% when schwertmannite was reused for 12 cycles. This result clearly indicated that schwertmannite retained as high as 80.0% of its catalyzing capacity even after 12 cycles of reuse, which suggested that schwertmannite could be repeatedly used as a Fenton-like catalyst. It could be seen from Fig. 11b that the concentration of leached Fe was 2.72 mg L^{-1} before recycling schwertmannite. During the 12 cycles of schwertmannite, the leaching amount of Fe remained in a range of 0.38–0.58 mg L^{-1}, which is acceptable in accordance with European Union discharge standards (<2 mg L^{-1}).[49]

The structure and morphology of schwertmannite after 12 times of repeated use were also investigated. XRD spectra shown in Fig. 2a displayed that the XRD patterns of repeatedly

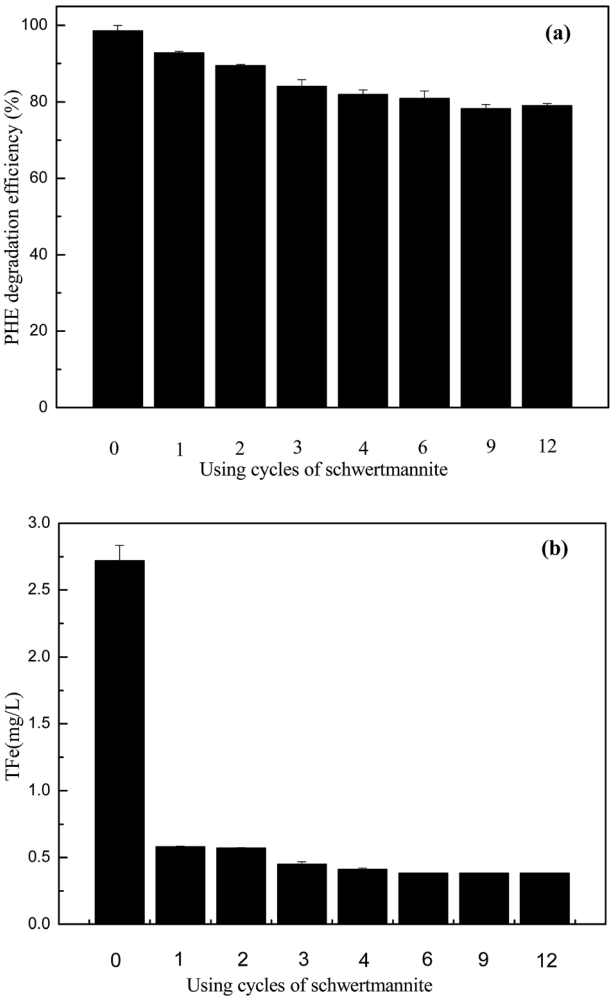

Fig. 11 Changes of phenanthrene degradation efficiency (a) and dissolution of Fe-ion (b) during a multi-cycle experiment with repeated uses of biosynthetic schwertmannite. Experimental conditions were $[phenanthrene]_0 = 1$ mg L^{-1}, $[schwertmannite]_0 = 1$ g L^{-1}, $[H_2O_2]_0 = 200$ mg L^{-1}, solution initial pH = 3.0, and reaction time of 12 h in each cycle.

used schwertmannite for 12 times still matched the standard diffraction data for schwertmannite (JCPDS no. 47-1775). The FTIR spectrum of newly biosynthesized schwertmannite was shown in the Fig. S4.† It can be seen that the absorption peaks at wavelength 3217 cm^{-1} were attributed to the stretching of free/bound hydroxyl groups; the absorption peaks at wavelength 1631 cm^{-1} were assigned to the O–H vibrations of H_2O molecules or structural OH groups; the γ_3 and γ_1 vibration of SO_4^{2-} were represented in the wavenumbers of 1117 and 982 cm^{-1}, respectively; the absorption peaks at wavelength 609 cm^{-1} were caused by the vibration of SO_4^{2-}; the absorption peaks at wavelength 483 cm^{-1} were ascribed to Fe–O bond vibration. All functional groups represented in the IR spectra were the same as that of schwertmannite.[21,23,38] The FTIR spectrum of repeatedly used schwertmannite for 12 times was in the agreement with those of newly biosynthesized schwertmannite. These results indicated that the Fenton-like reaction barely damaged the structure and functional groups of schwertmannite. Although some studies pointed out that schwertmannite is a metastable mineral and it can easily transform into goethite under oxidation conditions,[9] results of the present study showed that schwertmannite is an excellent Fenton-like catalyst for the degradation of phenanthrene and its mineral structure did not change during its repeated use.

4. Conclusion

The schwertmannite biosynthesized by *Acidithiobacillus ferrooxidans* is a poorly crystalline iron oxyhydroxysulfate with a high specific surface area. This biosynthetic schwertmannite can be used as a catalyst for the degradation of phenanthrene by the heterogeneous Fenton-like reaction. The degradation efficiency of phenanthrene was above 99.0% within 3–5 h reaction, under the reaction conditions of H_2O_2 200 mg L^{-1}, schwertmannite 1 g L^{-1}, phenanthrene 1 mg L^{-1} and pH 3.0–4.5. The degradation of phenanthrene by biosynthetic schwertmannite/H_2O_2 reaction was mainly *via* a surface mechanism, in which phenanthrene can be readily adsorbed on the surface of schwertmannite and then oxidized by hydroxyl radical produced from H_2O_2 decomposition. The Fenton-like degradation of phenanthrene resulted in a change of Fe^{2+}/Fe^{3+} species on the surface of biosynthetic schwertmannite. Moreover, phthalates, octadecanoic acid and 9,10-phenanthraquinone were the main intermediate compounds during the transformation of phenanthrene in biosynthetic schwertmannite/H_2O_2 system, and all the intermediate compounds can be mineralized finally. In the presence of inorganic anions, phenanthrene degradation was suppressed to some degree in a sequence of $SO_4^{2-} > H_2PO_4^- > NO_3^- > Cl^-$. The repeated use of schwertmannite as a Fenton-like catalyst did not significantly change its catalytic activity, mineral structure, and function groups, indicating that biosynthetic schwertmannite had a good stability and reusability as a Fenton-like catalyst for phenanthrene degradation. Therefore, biosynthetic schwertmannite is an excellent catalyst for the degradation of phenanthrene in heterogeneous Fenton-like reactions.

Acknowledgements

The authors would like to thank the financial support from National Natural Science Foundation of China (21477055, 21637003, and 21307059).

Note and references

1 M. S. García-Falcón and J. Simal-Gándara, *Food Addit. Contam.*, 2005, **22**, 791–797.
2 L. Rey-Salgueiro, E. Martínez-Carballo, M. S. García-Falcón, C. Gonzalez-Barreiro and J. Simgal-Gandara, *Food Chem.*, 2009, **115**, 814–819.
3 S. Gan and H. K. Ng, *Chem. Eng. J.*, 2012, **180**, 1–8.
4 M. S. García-Falcón, B. Soto-González and J. Simal-Gándara, *Environ. Sci. Technol.*, 2006, **40**, 759–763.
5 M. Usman, P. Faure, C. Ruby and K. Hanna, *Appl. Catal., B*, 2012, **117**, 10–17.
6 J. H. Ramirez, F. J. Maldonado-Hódar, A. F. Pérez-Cadenas, C. Moreno-Castilla, C. A. Costa and L. M. Madeira, *Appl. Catal., B*, 2007, **75**, 312–323.
7 R. Li, Y. Gao, X. Jin, Z. Chen, M. Megharaj and R. Naidu, *J. Colloid Interface Sci.*, 2015, **438**, 87–93.
8 J. J. Pignatello, E. Oliveros and A. MacKay, *Crit. Rev. Environ. Sci. Technol.*, 2006, **36**, 1–84.
9 E. D. Burton, S. G. Johnston, K. M. Watling, R. T. Bush, A. F. Keene and L. A. Sullivan, *Environ. Sci. Technol.*, 2010, **44**, 2016–2021.
10 J. D. Laat, G. T. Le and B. Legube, *Chemosphere*, 2004, **55**, 715–723.
11 R. Maciel, G. L. Sant'Anna Jr and M. Dezotti, *Chemosphere*, 2004, **57**, 711–719.
12 S. S. Lin and M. D. Gurol, *Environ. Sci. Technol.*, 1998, **32**, 1417–1423.
13 S. H. Tian, Y. T. Tu, D. S. Chen, X. Chen and Y. Xiong, *Chem. Eng. J.*, 2011, **169**, 31–37.
14 S. Lomnicki, H. Truong, E. Vejerano and B. Dellinger, *Environ. Sci. Technol.*, 2008, **42**, 4982–4988.
15 I. S. X. Pinto, P. H. V. V. Pacheco, J. V. Coelho, E. Lorencon, J. D. Ardisson, J. D. Fabris, P. P. Souza, K. W. H. Krambrock, L. C. A. Oliveira and M. C. Pereira, *Appl. Catal., B*, 2012, **119**, 175–182.
16 X. Xue, K. Hanna, M. Abdelmoula and N. Deng, *Appl. Catal., B*, 2009, **89**, 432–440.
17 K. Toda, T. Tanaka, Y. Tsuda, M. Ban, E. P. Koveke, M. Koinuma and S. I. Ohira, *J. Hazard. Mater.*, 2014, **278**, 426–432.
18 J. M. Bigham, U. Schwertmann, L. Carlson and E. Murad, *Geochim. Cosmochim. Acta*, 1990, **54**, 2743–2758.
19 J. M. Bigham, L. Carlson and E. Murad, *Mineral. Mag.*, 1994, **58**, 641–648.
20 Y. Liao, L. Zhou, J. Liang and H. Xiong, *Mater. Sci. Eng., C*, 2009, **29**, 211–215.
21 J. M. Bigham, U. Schwertmann, S. J. Traina, R. L. Winland and M. Wolf, *Geochim. Cosmochim. Acta*, 1996, **60**, 2111–2121.

22 S. Regenspurg and S. Peiffer, *Appl. Geochem.*, 2005, **20**, 1226–1239.
23 S. Regenspurg, A. Brand and S. Peiffer, *Geochim. Cosmochim. Acta*, 2004, **68**, 1185–1197.
24 S. Paikaray, J. Göttlicher and S. Peiffer, *Chem. Geol.*, 2011, **283**, 134–142.
25 F. Liu, J. Zhou, S. Zhang, L. Liu, L. Zhou and W. Fan, *PLoS One*, 2015, **10**, e0138891.
26 Z. Li, J. Liang, S. Bai and L. Zhou, *Acta Sci. Circumstantiae*, 2011, **31**, 460–467.
27 H. Duan, Y. Liu, X. Yin, J. Bai and J. Qi, *Chem. Eng. J.*, 2016, **283**, 873–879.
28 W.-M. Wang, J. Song and X. Han, *J. Hazard. Mater.*, 2013, **262**, 412–419.
29 L. Xu and J. Wang, *Appl. Catal., B*, 2012, **123**, 117–126.
30 B. A. Manning, S. E. Fendorf and S. Goldberg, *Environ. Sci. Technol.*, 1998, **32**, 2383–2388.
31 P. Nkedi-Kizza, P. S. C. Rao and A. G. Hornsby, *Environ. Sci. Technol.*, 1985, **19**, 975–979.
32 Z.-R. Lin, L. Zhao and Y.-H. Dong, *Chemosphere*, 2015, **141**, 7–12.
33 C. P. Huang and Y. H. Huang, *Appl. Catal., A*, 2008, **346**, 140–148.
34 T. Rhadfi, J. Y. Piquemal, L. Sicard, F. Herbst, E. Briot, M. Benedetti and A. Atlamsani, *Appl. Catal., A*, 2010, **386**, 132–139.
35 A. A. Burbano, D. D. Dionysiou, M. T. Suidan and T. L. Richardson, *Water Res.*, 2005, **39**, 107–118.
36 A. Georgi, A. Schierz, U. Trommler, C. P. Horwitz, T. J. Collins and F. D. Kopinke, *Appl. Catal., B*, 2007, **72**, 26–36.
37 I. A. Katsoyiannis, T. Ruettimann and S. J. Hug, *Environ. Sci. Technol.*, 2008, **42**, 7424–7430.
38 Z. Xu, J. Liang and L. Zhou, *J. Alloys Compd.*, 2013, **546**, 112–118.
39 H. S. Park, Y. C. Lee, B. G. Choi, Y. S. Choi, J. W. Wang and W. H. Hong, *Small*, 2010, **6**, 290–295.
40 B. David and P. Boule, *Chemosphere*, 1993, **26**, 1617–1630.
41 H. Jia, J. Zhao, X. Fan, K. Dilimulati and C. Wang, *Appl. Catal., B*, 2012, **123**, 43–51.
42 M. Yin, Z. Li, J. Kou and Z. Zou, *Environ. Sci. Technol.*, 2009, **43**, 8361–8366.
43 O. T. Woo, W. K. Chung, K. H. Wong, A. T. Chow and P. K. Wong, *J. Hazard. Mater.*, 2009, **168**, 1192–1199.
44 T. Cajthaml, P. Erbanová, V. Šašek and M. Moeder, *Chemosphere*, 2006, **64**, 560–564.
45 W. Luo, L. H. Zhu, N. Wang, H. Q. Tang, M. J. Cao and Y. B. She, *Environ. Sci. Technol.*, 2010, **44**, 1786–1791.
46 H. Gallard and J. D. Laat, *Water Res.*, 2000, **34**, 3107–3116.
47 Y. Liu, A. Zhou, Y. Gan and X. Li, *J. Hazard. Mater.*, 2016, **308**, 187–191.
48 J. D. Laat and T. G. Le, *Appl. Catal., B*, 2006, **66**, 137–146.
49 S. Sabhi and J. Kiwi, *Water Res.*, 2001, **35**, 1994–2002.

